Nanoscale Advances

ROYAL SOCIETY OF CHEMISTRY

PAPER

Cite this: *Nanoscale Adv.*, 2023, **5**, 2794

Poly(2-oxazoline)-based core cross-linked star polymers: synthesis and drug delivery applications†

Nedah Alkattan, [ab] Noura Alasmael, [c] Viko Ladelta, [a] Niveen M. Khashab *[c] and Nikos Hadjichristidis *[a]

Poly(2-oxazoline)s (POxs) are promising platforms for drug delivery applications due to their biocompatibility and stealth properties. In addition, the use of core cross-linked star (CCS) polymers based on POxs is expected to enhance drug encapsulation and release performances. In this study, we employed the "arm-first" strategy to synthesize a series of amphiphilic CCS [poly(2-methyl-2-oxazoline)]$_n$-*block*-poly(2,2′-(1,4-phenylene)bis-2-oxazoline)-cross-link/copolymer-(2-*n*-butyl-2-oxazoline)s (PMeOx)$_n$-*b*-P(PhBisOx-*cl*/*co*-ButOx)s by using microwave-assisted cationic ring-opening polymerization (CROP). First, PMeOx, as the hydrophilic arm, was synthesized by CROP of MeOx using methyl tosylate as the initiator. Subsequently, the living PMeOx was used as the macroinitiator to initiate the copolymerization/core-crosslinking reaction of ButOx and PhBisOx to form CCS POxs having a hydrophobic core. The molecular structures of the resulting CCS POxs were characterized by size exclusion chromatography and nuclear magnetic resonance spectroscopy. The CCS POxs were loaded with the anti-cancer drug doxorubicin (DOX), and the loading was detected by UV-vis spectrometry, dynamic light scattering, and transmission electron microscopy. *In vitro* studies showed that DOX release at pH 5.2 was faster than that at pH 7.1. The *in vitro* cytotoxicity study using HeLa cells revealed that the neat CCS POxs are compatible with the cells. In contrast, the DOX-loaded CCS POxs exhibited a cytotoxic effect in a concentration-dependent manner in HeLa cells, which strongly supports that the CSS POxs are potential candidates for drug delivery applications.

Received 23rd February 2023
Accepted 5th April 2023

DOI: 10.1039/d3na00116d

rsc.li/nanoscale-advances

Introduction

In the last decade, a wide range of polymeric nanoparticles has received significant attention for drug delivery applications.[1] One example of these drug carriers is polymeric micelles, which are formed in an aqueous solution by the self-assembly of amphiphilic copolymers.[2–4] The hydrophilic blocks of the copolymer stabilize the assemblies in the aqueous medium, while the hydrophobic block of the copolymer traps the hydrophobic drug molecules in their cores. Due to these features, hydrophobic drugs can be encapsulated inside the micelles of amphiphilic copolymers in a concentration higher than their water solubility. However, polymeric micelles have a significant drawback which is instability under external stimuli such as high temperature or low concentrations.[5–7]

Such drawbacks can be tackled by employing unimolecular polymeric micelles/containers that have core–shell architectures such as dendrimers,[8] hyperbranched polymers,[9] and star polymers.[10–12] The usage of dendrimers and hyperbranched polymers is constrained due to complex synthetic processes. In addition, the small free volume of the dendritic cavity limits the hydrophobic drug encapsulation capacity.[8,13] In contrast, star polymers can be accessed through facile and straightforward controlled polymerization processes. Such processes facilitate the synthesis of star polymers having a core with a higher free volume and encapsulate higher content of hydrophobic drugs.[14] Star polymer-based micelles are also more stable than those formed by amphiphilic linear copolymers because of their covalently core.

Star polymers can be synthesized by three synthetic strategies: core-first strategy, grafting-onto strategy, and arm-first strategy. The core first strategy uses a multifunctional initiator, which has the advantage of generating well-defined stars with a predictable number of arms. However, this approach produces a small core, leading to low drug loading capacity.[14,15] The grafting-onto strategy is performed by controlled

[a]*Polymer Synthesis Laboratory, Chemistry Program, KAUST Catalysis Center, Physical Sciences and Engineering Division, King Abdullah University of Science and Technology (KAUST), Thuwal 23955, Saudi Arabia. Tel: +966-(0)12-8080789*

[b]*Refining and Petrochemical Technologies Institute, King Abdulaziz City for Science and Technology, P. O Box 6086, Riyadh 11442, Saudi Arabia*

[c]*Smart Hybrid Materials (SHMs) Laboratory, Chemistry Program, Advanced Membranes and Porous Materials Center, King Abdullah University of Science and Technology (KAUST), Thuwal 23955-6900, Saudi Arabia. E-mail: nikolaos.hadjichristidis@kaust.edu.sa; Tel: +966-(0)12-8080789*

† Electronic supplementary information (ESI) available: Fig. S1 to S12 (^{1}HNMR, GPC, DLS, TEM images, *in vitro* drug release, and cytotoxicity studies). Eqn (S1)–(S3) and Scheme S1 (drug loading and drug release). See DOI: https://doi.org/10.1039/d3na00116d

polymerization to prepare the arm and then attaching it to a core having a multifunctional linking agent *via* a coupling reaction. This method gives the ability to manipulate both the arm length and the core size. However, this method is less preferred because it requires multiple purification steps and prolonged reaction times.[16]

The third strategy is called the arm-first strategy (core cross-linked strategy). First, the linear living macroinitiator (the arm) is prepared and then used to initiate the polymerization of the difunctional cross-linker monomer to afford a unique three-dimensional core cross-linked star (CCS) polymer structure. This strategy allows the synthesis of star polymers with high numbers of well-defined arms as well as a larger cross-linked core that can encapsulate higher amounts of drug.[17] CCS polymers have a huge number of potential in biomedical applications and unique properties,[18–20] especially when they consist of biodegradable/biocompatible polymeric backbones such as poly(2-oxazoline) (POxs).

POxs are mono-substituted derivatives of poly(amides), discovered in 1966 by four independent research groups.[21–24] POxs are often recognized as pseudo-polypeptides because of their structural analogies with natural polypeptides.[25] In addition, POxs offer some advantages compare to poly(ethylene glycol) (PEG), particularly as drug carriers.[26] One of the most significant advantages of POxs over PEG is that the functionalization of POxs (on the side chain or at the chain end) is easier than that of PEG.[26] Moreover, employing POxs increases the solubility, bioavailability, drug loading capacity, and drug circulation in the blood,[27] and reduces toxicity.[28,29]

There are different methods that have been published in the literature to synthesize POxs. The main method to synthesize POxs is by living cationic ring-opening polymerization (CROP) of 2-oxazolines. Due to the slow polymerization rate, CROP of 2-oxazolines is usually carried out under microwave irradiation to accelerate the propagation reaction and reduce the polymerization time.[30] The polymerization is initiated by an electrophilic initiator such as tosylate, triflates, alkyl halides, and Lewis acids.[26,31] CROP of 2-oxazolines allows the synthesis of well-defined homo- and copolymers of POxs[26] with narrow molecular weight distribution, a high degree of polymerization control and complex architectures.[32]

Recently, Becer and his coworkers reported the synthesis of CCS POxs *via* the arm-first strategy.[33] They synthesized poly(2-ethyl-2-oxazoline) arms in various lengths and cross-linked them with a bis-2-oxazoline cross-linker (consisting of two units of 2-isopropenyl-2-oxazoline connected by a sulfur bond) to create star-shaped polymers. However, the cross-linker that they used is not commercially available and less hydrophobic. Moreover, the drug encapsulation potential of the resulting CCS POxs was not evaluated by encapsulating the actual drug but by using dihydroxyanthraquinone (DHA) as a model compound.

This work reports a series of well-defined CCS (PMeOx)$_n$-*b*-P(PhBisOx-*cl*/*co*-ButOx)s synthesized *via* the "arm first" strategy. The polymers consist of PMeOx as the hydrophilic arm and P(PhBisOx-*cl*/*co*-ButOx) (*cl*: cross-link) as the hydrophobic core. PhBisOx is commercially available and contains an aromatic group that brings in hydrophobicity as well as simplicity as can be probed by UV-vis spectrometry. Moreover, the use of ButOx as a hydrophobic comonomer can expand the core size and increase the drug encapsulation capacity of CCS POxs. The molecular structure of the CCS POxs was characterized by SEC and NMR. DLS and TEM reveal that the CCS POxs formed unimolecular micelles in water. Drug loading capacity and *in vitro* release properties of the CCS POxs were studied by encapsulating doxorubicin (DOX), a common anti-cancer drug, into the polymer micelles. The results show that CCS (PMeOx)$_n$-*b*-P(PhBisOx-*cl*/*co*-ButOx)s are potential candidates for drug delivery applications.

Experimental section

Materials

2-Methyl-2-oxazoline (98%) and 2-*n*-butyl-2-oxazoline were distilled over barium oxide (BaO) and stored in a dry flask under argon. Methyl *p*-toluenesulfonate (98%), (Sigma-Aldrich), and 2,2′-(1,4-phenylene)bis-2-oxazoline (PhBisOx) (Tokyo Chemical Industry, TCI chemicals) were used as received. The solvents (diethyl ether and dichloromethane, DCM) from (VWR chemicals), dimethyl sulfoxide (DMSO: Aldrich, 99.9%), and triethylamine (TEA: Aldrich, 98%) were used as received. Deionized water (Milli-Q water) was used to terminate the polymerization. Human cervical cancer cells (HeLa) were purchased from the American Type Culture Collection (ATCC, Manassas, VA, USA). Dulbecco's modified Eagle's medium (DMEM), fetal bovine serum (FBS), penicillin–streptomycin, 1× phosphate-buffered saline (PBS), 0.025% trypsin–EDTA, and distilled water were obtained from Gibco. T75 cell culture flasks were purchased from Thermo Scientific. 96-well plates were procured from Corning Incorporated. The cell cytotoxicity assay solution was obtained from Abcam. Doxorubicin hydrochloride (DOX·HCL) was purchased from TCI Chemicals.

Synthesis of poly(2-methyl-2-oxazoline)(PMeOx)

As an example, the synthesis of the (PMeOx) (8400 g mol^{-1}) is given. In a glovebox under an argon (Ar) atmosphere, 2-methyl-2-oxazoline (4.0 g, 47.0 mmol) and methyl tosylate (87.5 mg, 0.47 mmol) were dissolved in dichloromethane DCM (8.0 mL) to obtain a 4 M reaction concentration. This solution was transferred into four microwave vials (3.0 mL each). The vials were placed in a microwave reactor and heated for 7 min at 140 °C. We followed all the safety precautions when performing the experiment. PMeOx was obtained as a white solid with a 90% yield. ^{1}H NMR (500 MHz, $CDCl_3$) δ ppm 3.65–3.32 (4H, t, backbone protons, peak g), 2.96–2.93 (3H, s, initiator protons, peak e), 2.17–1.98 (3H, s, methyl group, peak f) of side-chain of PMeOx. $M_{n,\mathrm{NMR}}$ (PMeOx) = 8400 g mol^{-1}.

Synthesis of the core cross-linked star (PMeOx)$_n$-*b*-P(PhBisOx-*cl*/*co*-ButOx) by microwave-assisted CROP

As an example, the synthesis of the (PMeOx)$_{59}$-*b*-P(PhBisOx-*cl*/*co*-ButOx) star is given. In a glovebox under an Ar atmosphere, 2,2′-(1,4-phenylene)bis-2-oxazoline (PhBisOx) (381 mg, 1.76 mmol) and 2 mL DCM were added to one of the aforementioned

vials containing living PMeOx at ~40 °C. The mixture was heated again in a microwave reactor for 30 min at 140 °C, resulting in $(PMeOx)_n$-*b*-PhBisOx. The cross-linker and comonomer, PhBisOx (381 mg, 1.76 mmol) and (ButOx (0.17 mL, 1.17 mmol)), were added to each of the remaining vials containing living PMeOx and kept for 30 min under microwave irradiation to afford $(PMeOx)_{59}$-*b*-P(PhBisOx-*cl*/*co*-ButOx). After completion of the polymerization, the yellowish polymer solutions were quenched by adding water and finally precipitated in cold diethyl ether and dried under vacuum at 45 °C. The product was obtained as a white powder with a 97% yield. ^{1}H NMR (500 MHz, $CDCl_3$) δ ppm 8.01 (s, 4H, aromatic proton, peak h), 3.58–3.35 (t, 4H, backbone protons, peak g), 2.46–2.22 (t, 2H, peak d), 2.21–2.00 (s, 3H, peak f), 1.64–1.0 (m, 2H, peak c), 1.40–1.22 (m, 2H, peak b), and 0.99–0.78 (t, 3H, peak a).

In vitro study of core-cross linked star (CCS) polymer

DOX-loading. DOX·HCl (0.5 mg, 0.5 mL) was first neutralized with two equivalents of triethylamine (TEA) in DMSO for 2 h to obtain the pristine DOX (hydrophobic). The DOX solution was added to the CCS polymer solution (5.0 mg, 1.5 mL DMSO) and stirred for 30 minutes. Then, the DOX-polymer solution was added dropwise into 3 mL of deionized water under stirring for 4 h. The organic solvent and free drug were removed by dialysis (MWCO 3500) against deionized water for 24 h (the dialysis medium was changed three times). The solution was either lyophilized in the dark or used directly for measurement. The concentration and loading efficiency of DOX in the CCS polymers were estimated by measuring the absorbance at 485 nm against a calibration curve based on the UV-vis spectra. The drug loading content (DLC) and the drug loading efficiency (DLE) were calculated according to the following eqn (1) and (2);

$$\mathrm{DLC} = \frac{\text{Weight of loaded drug}}{\text{Weight of polymer used}} \times 100 \quad (1)$$

$$\mathrm{DLE} = \frac{\text{Weight of loaded drug}}{\text{Total weight of drugs used}} \times 100 \quad (2)$$

DOX release from CCS polymers. DOX-loaded CCS polymers were treated at 37 °C in buffer solution PBS (pH = 5.2 and 7.1). DOX-loaded CCS polymers (800 μL) were placed in the dialysis membrane and dialyzed against PBS solution (13 mL). 1 mL of the aliquot from the release medium was taken at a specific time interval, and the absorbance of each sample was recorded at 485 nm to determine the concentration of DOX released from the CCS polymers.

General cell culture. HeLa cells were maintained in Dulbecco's modified Eagle's medium (DMEM) supplemented with 10% (v/v) FBS and 1% (v/v) penicillin–streptomycin at 37 °C with 5% CO_2 and 95% humidity within a CO_2 incubator. Frozen vials of cell line were rapidly thawed in a 37 °C water bath with gentle agitation and placed immediately in 15 mL of fresh, pre-warmed growth media. The cells were routinely passaged when they reached approximately 70–80% confluence.

Cytotoxicity study. Cell viability assays were performed to evaluate the biocompatibility of blank polymers. HeLa cells were plated at a density of 5×10^3 or 3×10^3 per well in a clear flat-bottomed 96-well plate and incubated overnight to attach. Polymer stock solutions were dissolved in sterile distilled water and used to create various concentrations. Cells were incubated with 200 μL per well of cell culture media containing different concentrations of blank polymer (1, 10, 25, 50, 100, 200, and 300 μg mL^{-1}) for 24 and 48 h. The negative control was only cells with media, and no polymer was added. All media containing the treatments of blank polymers were discarded and replaced with 100 μL fresh media, then 20 μL of cytotoxicity assay solution was added to each well, and the plate was then placed in a shaker for 30 seconds. Cells were incubated for 3.5 hours at 37 °C with 5% CO_2. According to the manufacturer's instructions, a microplate reader (xMark™ microplate, Varioskan LUX, Thermos Scientific) was used to monitor the absorbance ratio at two wavelengths, 570 nm and 605 nm.

Instruments

Polymerizations were performed in a single-mode microwave reactor Ermys Liberator (Biotage) utilizing capped reaction vials. All vials are equipped with a noninvasive IR sensor (accuracy ±1%). All microwave-assisted polymerizations were performed with temperature control. The vials were heated at 140 °C and allowed to cool to room temperature under an Ar atmosphere.

Size exclusion chromatography (SEC)

SEC analysis was performed on an Agilent 1260 infinity-size exclusion chromatography instrument equipped with a 1200 HPLC pump and Agilent 1260 system fitted with refractive index (RID) and UV-vis detectors. Two identical PLgel columns (10 μm, MIXED-C) and one guard column were used. *N*,*N*-Dimethylformamide (DMF) with 0.005 M LiCl was used as the mobile phase at a flow rate of 1 mL min^{-1}. The dispersity ($M_w/M_n = Đ$) was determined using a polystyrene standard calibration curve. The column and flow path temperature were controlled at 45 °C. Polymer solutions with a concentration ~2 mg mL^{-1} were filtered through a 0.22 μm nylon membrane and injected into the SEC instrument at an injection volume of 200 μL.

Preparative SEC

A Next LC-9130 system with a 10 mL sample injection loop, a LaboACE 5060/7080 differential refractometer detector, a UV-vis 4ch 400LA ultraviolet detector, a fraction collector FC-3310, JAIGEL-3HR (20μϕ × 600) and JAIGEL-4HR (20μϕ × 600) preparative columns, and a JAIGEL-HR-P precolumn were used for preparative SEC. DMF containing 0.1 gL^{-1} of LiCl was used as the mobile phase. The crude polymer injection had a concentration of around 50 mg mL^{-1}. At room temperature, the system was run at a flow rate of 8 mL min^{-1}.

Nuclear magnetic resonance (NMR)

^{1}H and ^{13}C NMR measurements were performed at 25 °C using Bruker AVANCE III 500 MHz NMR spectrometers in $CDCl_3$, and

tetramethylsilane (TMS) was used as the internal standard. Chemical shifts are given as δ (ppm) values relative to TMS or residual solvent.

Dynamic light scattering (DLS)

Each of the CCS POxs that were synthesized according to the above procedures was dissolved in water at a concentration of 2 mg mL^{-1}. Then, each solution was passed through a 0.22 μm nylon membrane filter before analysis. DLS measurements were performed in triplicate on a Malvern Zetasizer Nano ZS instrument equipped with a 30 mW He–Ne laser light of 632.8 nm wavelength with a scattering angle of 90° angle. The measurements were carried out in water at room temperature.

Transmission electron microscopy (TEM)

TEM images were acquired using a Titan ST (Thermo Fisher) instrument operating at 300 kV acceleration voltage. For sample preparation, a drop of solution was placed on a carbon-coated copper grid, blotted with filter paper, and allowed to dry under ambient conditions.

UV-visible spectrophotometry

The absorption spectra of the DOX-loaded polymers were recorded using a Shimadzu UV-vis spectrophotometer (UV-2600). The DOX-loaded polymers (1 mg mL^{-1}) were dissolved in water and added to a disposable cuvette at room temperature.

Results and discussion

Synthesis of amphiphilic core cross-linked star POxs

CCS polymers reported in this work were synthesized *via* the "arm first strategy" by microwave-assisted CROP. Living CROP allows the synthesis of well-defined arms and cores[34,35] of CCS poly(2-oxazoline) *via* a sequential copolymerization/cross-linking reaction (Scheme 1). PMeOx (the hydrophilic arm) is soluble in a wide range of organic solvents as well as in water, while the hydrophobic core P(PhBisOx-*cl*/*co*-ButOx) is soluble in DCM. Therefore, DCM was used as the solvent for polymerization in a closed reaction vial under microwave irradiation at 140 °C.

First, 2-methyl-2-oxazoline (MeOx) was polymerized by using *p*-toluenesulfonate (methyl tosylate) as the initiator in DCM at

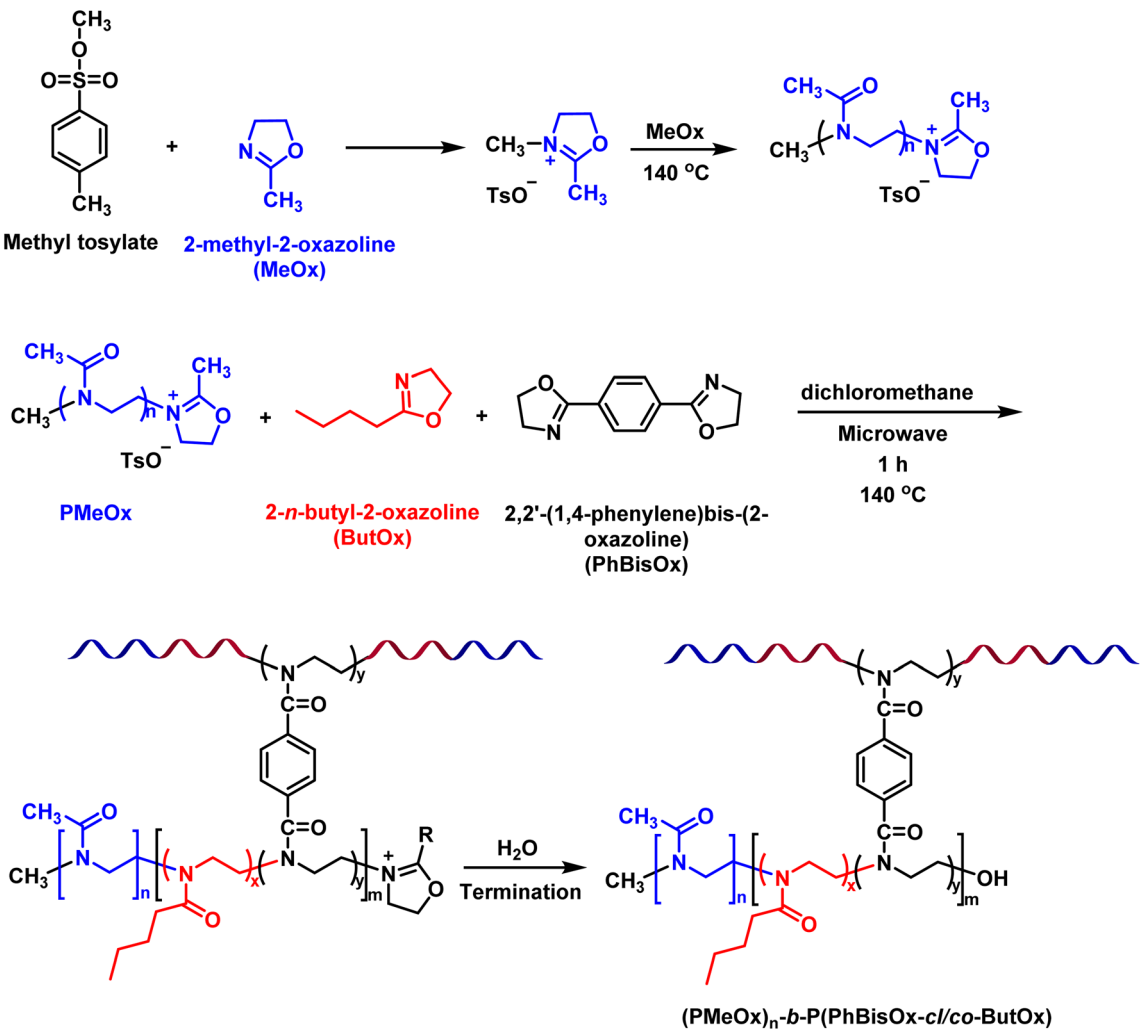

Scheme 1 Synthetic route to prepare CCS $(PMeOx)_n$-*b*-P(PhBisOx-*cl*/*co*-ButOx) by microwave-assisted CROP.

140 °C under microwave irradiation (Scheme 1).[30] After 7 min, the core of the CCS polymers was synthesized in one pot by the addition of PhBisOx (cross-linker) and ButOx (hydrophobic comonomer) to the living PMeOx solution (Scheme 1). Several CCS POxs were synthesized by varying the cross-linker and the hydrophobic monomer ratios, as listed in Table 1.

The conversion of the monomer to polymer and the degree of polymerization was monitored by ^{1}H NMR spectroscopy. For example, in the case of (PMeOx)$_{59}$-*b*-P(PhBisOx-*cl*/*co*-ButOx), the conversion of PMeOx was calculated by comparing the integral value of the two methylene peaks of the monomer (δ 3.46–3.34 ppm, h) and (δ 3.86–3.77 ppm, g) as shown in Fig. S1 (ESI†) with the one in the polymer (Fig. 1, black). After the polymerization, the two methylene peaks in the monomer (g and h) merged as a broad peak at 3.58–3.33 ppm (4H, –N–CH$_2$CH$_2$–, g) in the polymer. The conversion of MeOx to PMeOx reached at least 99% in 7 min, as proved by the disappearance of the monomer's peaks (g and h). Furthermore, the conversions of PhBisOx and ButOx into (PMeOx)$_n$-*b*-P(PhBisOx-*cl*/*co*-ButOx) were determined by the disappearance of the peaks of the 2-oxazoline ring at 4.48–4.43 ppm (k) and 4.11–4.06 ppm (m) as shown in Fig. S2 (ESI†) for PhBisOx, as well as the 2-oxazoline ring at 4.03–3.98 ppm (o) and 3.64–3.58 ppm (n) (Fig. S3, ESI†) for ButOx, followed by the appearance of new singlet broad peak at 3.58–3.33 ppm (Fig. 1; red, k, m for PPhBisOx and n, o for PButOx). The number average molecular weight (M_n) of PMeOx was calculated from ^{1}H NMR by comparing the integral value of the methyl protons of the tosylate initiator (Fig. 1, black, e) with

Table 1 Molecular characteristics of CCS (PMeOx)$_n$-*b*-P(PhBisOx-*cl*/*co*-ButOx) synthesized by CROP *via* the arm-first strategy

CCS polymers	[PhBisOx]$_0$	[ButOx]$_0$	PMeOx $M_{n,\ \mathrm{NMR}}$	WF[a] (PMeOx)	$M_{\mathrm{w,\ star}}$[b] (g L^{-1})	N_{arm}[c]	Star conv[d] (%)	$Đ$
PMeOx$_{100}$	—	—	8300	—	—	—	—	1.04
(PMeOx)$_{44}$-*b*-P(PhBisOx-*cl*/*co*-ButOx)	10	10	8300	0.99	373.000	44	83	1.22
(PMeOx)$_{106}$-*b*-P(PhBisOx-*cl*/*co*-ButOx)	10	25	8300	0.988	896.000	106	99	1.51
(PMeOx)$_{59}$-*b*-P(PhBisOx-*cl*/*co*-ButOx)	15	10	8200	0.99	493.000	59	76	1.12
(PMeOx)$_{62}$-*b*-P(PhBisOx-*cl*/*co*-ButOx)	15	25	8200	0.99	520.000	62	76	1.29

[a] Weigh fraction of PMeOx arms in the CCS POxs. [b] $M_{\mathrm{w,\ star}}$ determined by SEC-dual angle light scattering detector. [c] The average number of arms of the CCS POxs calculated from $N_{\mathrm{arm}} = (M_{\mathrm{w,\ star}} \times \mathrm{WF}_{\mathrm{arm}})/M_{\mathrm{w,\ arm}}$. [d] Star conversion was calculated from SEC trace using the following equation: $\text{star conversion}\% = \dfrac{\text{peak area of star polymer}}{\text{peak area of star polymer} + \text{peak area of unreacted arm}} \times 100$.

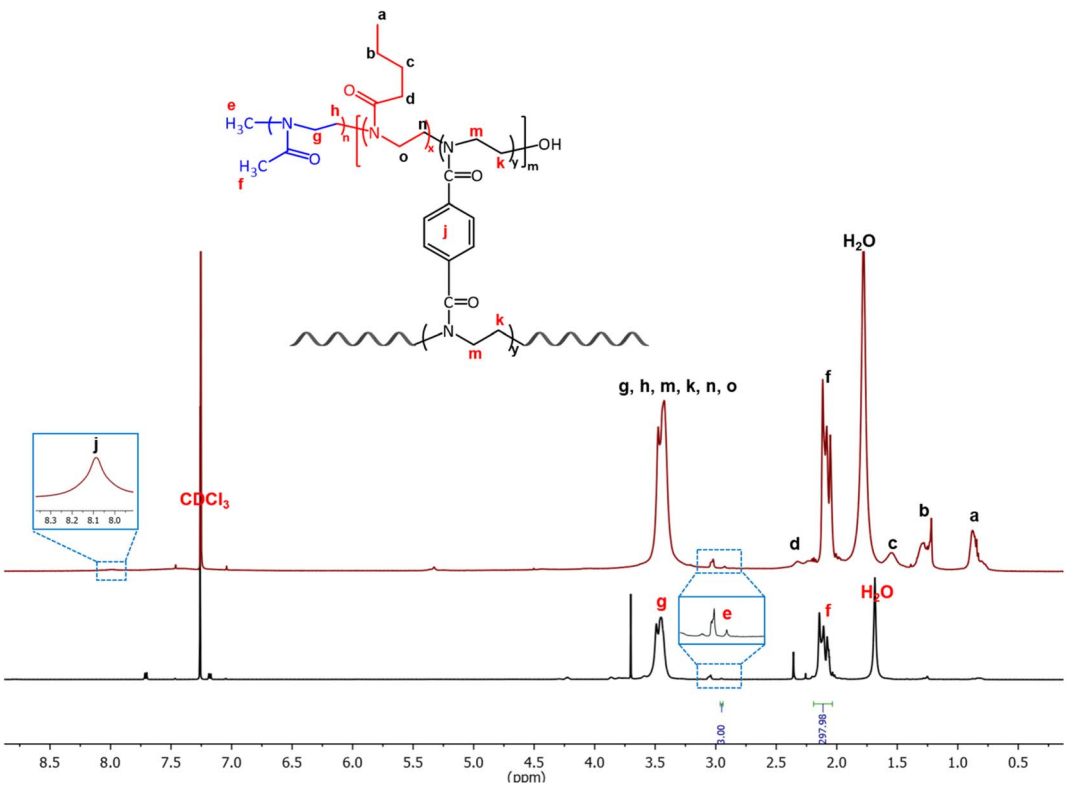

Fig. 1 ^{1}H NMR of the PMeOx arm (black) and (PMeOx)$_{59}$-*b*-P(PhBisOx-*cl*/*co*-ButOx) (red) (500 MHz, CDCl$_3$, 25 °C).

the integral value of the polymer backbone (Fig. 1, black, f or g and h).

The ^{13}C NMR spectrum also corroborates the structure of the CCS POxs, as shown in Fig. S4 (ESI†). The signal corresponding to the carbonyl carbon can be observed at 170 ppm. The peaks at 132 and 129 ppm correspond to the aromatic group of the cross-linker. The peaks of the polymer backbone (45 ppm) and the signals of the butyl side chain (13, 21, 27, and 32 ppm) were also observed.

The SEC trace of PMeOx (Fig. S5-black, ESI†) is monomodal and has narrow molar mass distribution ($Đ$ = <1.1), indicating the controlled/living CROP of MeOx. After the copolymerization/cross-linking reaction, the SEC trace showed the appearance of a new peak at the higher molecular weight position attributed to the CCS POxs (Fig. S5-red, ESI†). A small amount of residual PMeOx was observed after the cross-linking reaction. The relative percentage of the residual PMeOx arm (Table 1) can be calculated from the SEC chromatogram of unfractionated CCS POxs (eqn (1), ESI†). The unreacted PMeOx arm was separated from the CCS polymer by using preparative SEC with DMF as the mobile phase, resulting in monomodal CCS POxs (Fig. S5-blue, ESI†).

The pure CCS POxs after fractionation were recovered, and DMF was removed under high vacuum. Subsequently, residual water was removed from the polymer by lyophilization. All SEC traces show that the low molar mass polymeric products were removed after fractionation (Fig. 2(a–d)) and have narrow molar mass distribution ($Đ$ = 1.12–1.5). The high molar mass shoulders observed in the SEC traces of $(PMeOx)_{44}$-*b*-P(PhBisOx-*cl*/*co*-ButOx) with the initial feed ratios of PhBisOx and ButOx are 10 can be attributed to the star–star coupling formation favorable with the short arm (less steric hindrance). A similar phenomenon was also observed by Becer *et al.*[33] The average number of arms in the CCS POxs (Table 1) was calculated based on SEC, MDS-SEC, and ^{1}H NMR analysis of precursor polymers and star polymers, the details of the calculation can be found in eqn (2) (ESI†).

The effect of the feed ratio of ButOx monomeric units was studied by comparing $(PMeOx)_{44}$-*b*-P(PhBisOx-*cl*/*co*-ButOx) and $(PMeOx)_{106}$-*b*-P(PhBisOx-*cl*/*co*-ButOx), in which the initial feed ratio of PMeOX and cross-linker (Table 1) was fixed as 100 and 10, respectively. Fig. 2 shows that when the feed ratio of ButOx is increased from 10 to 25 nm, the M_n of the CCS POxs increases, and the number of arms increases from 44 to 106 (Table 1). A similar case also happened on $(PMeOx)_{59}$-*b*-P(PhBisOx-*cl*/*co*-ButOx) and $(PMeOx)_{62}$-*b*-P(PhBisOx-*cl*/*co*-ButOx), as shown in Fig. 2(b).

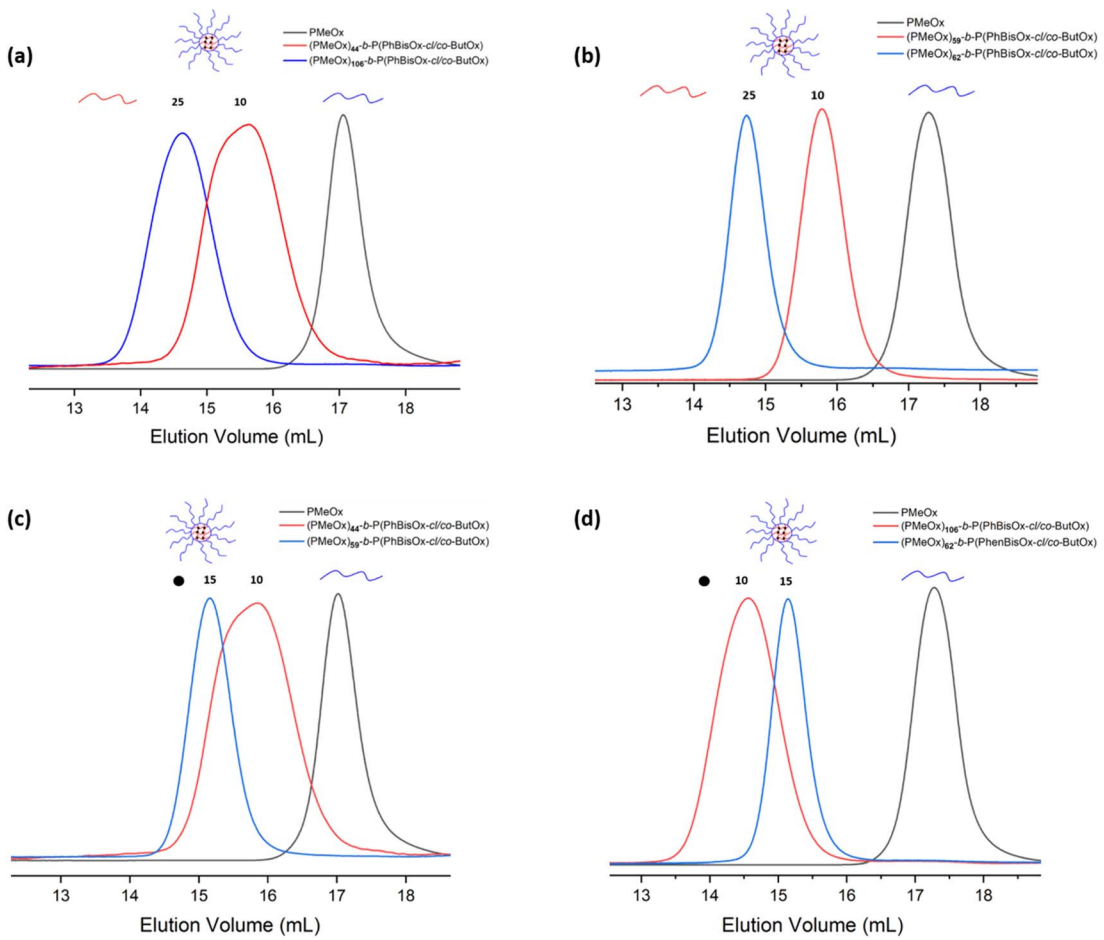

Fig. 2 (a) and (b) SEC traces of CCS polymers with different ratios of ButOx and (c) and (d) SEC traces for CCS polymers with different ratios of PhBisOx (DMF, 45 °C, PS standards).

It is very important to study the effect of the amount of cross-linker PhBisOx on the molecular characteristics of CCS POxs. As shown in Fig. 2(c), the molecular weight of the CCS POxs $(PMeOx)_{44}$-*b*-P(PhBisOx-*cl*/*co*-ButOx) and $(PMeOx)_{59}$-*b*-P(PhBisOx-*cl*/*co*-ButOx) increases when the feed ratio of ButOx is fixed as 10, and the feed ratio of PhBisOx is increased from 10 to 15 (Table 1). In contrast, for $(PMeOx)_{106}$-*b*-P(PhBisOx-*cl*/*co*-ButOx) and $(PMeOx)_{62}$-*b*-P(PhBisOx-*cl*/*co*-ButOx), in which the feed ratio of ButOx was fixed as 25, and the feed ratio of PhBisOx was increased from 10 to 15, a decrease in the molecular weight of the CCS star POxs was observed (Fig. 2(d)), due to the increased steric hindrance of the core. Increasing the feed ratio of PhBisOx to 20 or increasing the feed ratio of ButOx to 50 resulted in a polymeric gel that was insoluble in common organic solvents.

Dynamic light scattering (DLS) analysis was performed to study the particle size of the CCS POxs. The samples were dissolved in water with a concentration of 2 mg mL^{-1} at 25 °C and were filtered through a 0.22 μm nylon filter. The size of the CCS POxs was found to be in the range of 17–33 nm (Table 2). All CCS POx micelles showed a single-size distribution and low polydispersity values, as shown in (Fig. 3(a), black). TEM imaging (Fig. 3(b)) revealed that the morphology of CCS Pox micelles is spherical. The particle size of the CCS POxs increased when the ratio of the hydrophobic monomer (ButOx) increased from 10 to 25, as shown in Fig. S6(a) (ESI†). Similar to DLS, TEM images also showed that the size of the spherical micelles increases with the increase of ButOx (Fig. S6(b) and (c), ESI†).

In vitro study of CCS polymer micelles

DOX-loading. To evaluate the drug encapsulation capabilities of the synthesized CCS POxs, an anti-cancer drug, doxorubicin (DOX), was selected for *in vitro* studies. DOX is one of the most commonly used drugs to treat various cancers.[36] In this study, DOX·HCL (hydrophilic) was converted to DOX (hydrophobic) by neutralization with two equivalents of triethylamine (TEA) in DMSO for 2 h. The encapsulation of DOX occurs *via* physical entrapment due to the hydrophobic–hydrophobic interaction between DOX and the dense networks of the hydrophobic core of CCS POxs. Any unencapsulated DOX was removed by dialysis in water. After completion of the dialysis, stable DOX-loaded micelles were obtained and their particle size and morphology were analyzed by DLS and TEM.

Table 2 DLS results for free CCS POxs, DOX-loaded CCS POxs, and DOX encapsulation properties of CCS POxs

CCS polymers	d^a (nm)	PDI[b]	DLC (%)	DLE (%)
$(PMeOx)_{44}$-*b*-P(PhBisOx-*cl*/*co*-ButOx)	17	0.228	—	—
$(PMeOx)_{106}$-*b*-P(PhBisOx-*cl*/*co*-ButOx)	33	0.167	—	—
$(PMeOx)_{59}$-*b*-P(PhBisOx-*cl*/*co*-ButOx)	18	0.213	—	—
$(PMeOx)_{62}$-*b*-P(PhBisOx-*cl*/*co*-ButOx)	24	0.185	—	—
$(PMeOx)_{44}$-*b*-P(PhBisOx-*cl*/*co*-ButOx)-DOX	25	0.298	4.51	45.17
$(PMeOx)_{106}$-*b*-P(PhBisOx-*cl*/*co*-ButOx)-DOX	42	0.227	4.95	49.5
$(PMeOx)_{59}$-*b*-P(PhBisOx-*cl*/*co*-ButOx)-DOX	30	0.275	5.63	56.35
$(PMeOx)_{62}$-*b*-P(PhBisOx-*cl*/*co*-ButOx)-DOX	28	0.181	4.87	48.72

[a] The particle size (*d*). [b] Polydispersity of the CCS polymer solution, determined by DLS measurements (concentration: 1 mg mL^{-1}, temperature 25 °C). All measurements were repeated three times.

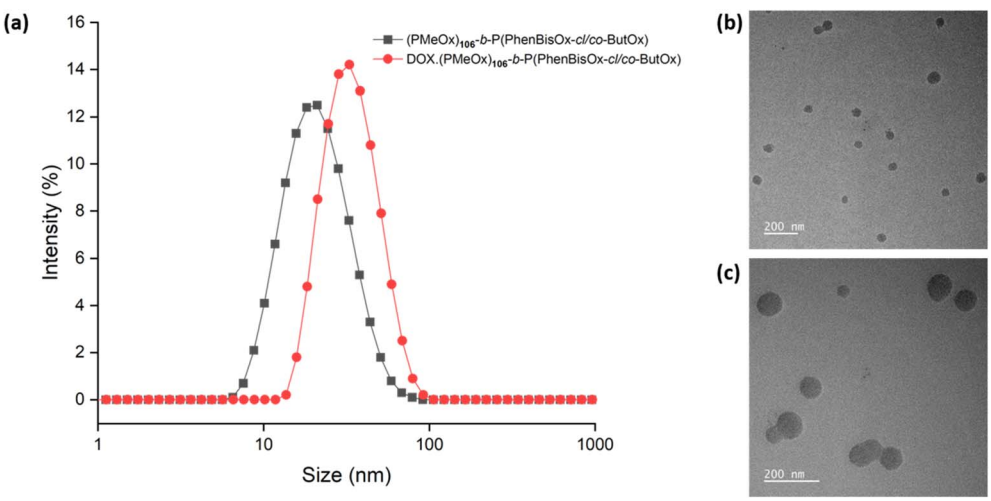

Fig. 3 (a) DLS traces of $(PMeOx)_{106}$-*b*-P(PhBisOx-*cl*/*co*-ButOx)(black) (concentration: 2 mg mL^{-1}) and DOX-loaded $(PMeOx)_{106}$-*b*-P(PhBisOx-*cl*/*co*-ButOx) (red) (concentration: 1 mg mL^{-1}) and TEM images of (b) $(PMeOx)_{106}$-*b*-P(PhBisOx-*cl*/*co*-ButOx) and (c) DOX-loaded $(PMeOx)_{106}$-*b*-P(PhBisOx-*cl*/*co*-ButOx).

DLS analysis reveals the change in the particle size of CCS POx micelles due to DOX encapsulation. For instance, the particle size of DOX loaded-$(PMeOx)_n$-*b*-P(PhBisOx-*cl*/*co*-ButOx) is bigger than that of the corresponding neat CCS POx micelles, as shown in Fig. 3(a), red. These results indicate that DOX is encapsulated in the core of the micelles. TEM images also support the formation of DOX-loaded CCS POx micelles, as shown in Fig. 3(c). The images show that the micelles are spherical for both neat- and DOX-loaded CCS POx micelles. Similar to the trend observed in DLS, TEM reveals that the size of micelles expanded about 6–9 nm after the encapsulation of DOX.

The drug loading capacity (DLC) and drug loading efficiency (DLE) were calculated based on a calibration curve (eqn (S3), ESI†) obtained by measuring the absorbance of free DOX in a water solution with known concentrations (Fig. S7, ESI†). The loading properties, particle size, and dispersity of the CCS POx micelles are summarized in Table 2. The DLC and DLE of the DOX-CCS conjugates increase when there is an increase in the hydrophobic core, which consist of the cross-linker (PhBisOx), and the hydrophobic monomer (ButOx).

In vitro release study

The *in vitro* release behavior of the DOX from CCS POxs $(PMeOx)_{106}$-*b*-P(PhBisOx-*cl*/*co*-ButOx) was investigated at two different simulated pH values (PBS with pH 7.1 and acidic pH 5.2) at a temperature of 37 °C (Fig. 4(a)). All CCS POxs showed a faster DOX release in acidic pH (5.2) than pH 7.1 because the amino group in DOX was protonated under acidic conditions. Thus, the solubility of DOX increases and the release is faster (Fig. S8, ESI†).[37] The drug release was slow within the first 24 h for both pH values, followed by the rise and sustained prolonged release for 48 h. Therefore, the feature of this system containing a cross-linked core makes this CCS POxs significant for controlled release and achieving targeted delivery, as illustrated in Scheme S1 (ESI†).

Cytotoxicity study of CCS POxs

In order to prove that the CCS POxs are non-toxic and biocompatible with the cells, their toxicity was studied *in vitro* by dissolving the CCS POxs in sterilized distilled water at different concentrations. Then, HeLa cells were incubated with cell culture media containing different concentrations of CCS POxs for 24 and 48 h. Cells with only media were used as a control with 100% viability. The results indicated that the biocompatibility of the CCS POxs is very high with HeLa cells up to 300 μg mL^{-1} with general cell viability ~100%, as shown in Fig. 4(b) for CSS $(PMeOx)_{106}$-*b*-P(PhBisOx-*cl*/*co*-ButOx) for 48 h. The results indicate that all CCS POxs are non-toxic and show no significant difference along the series. Cell proliferation was

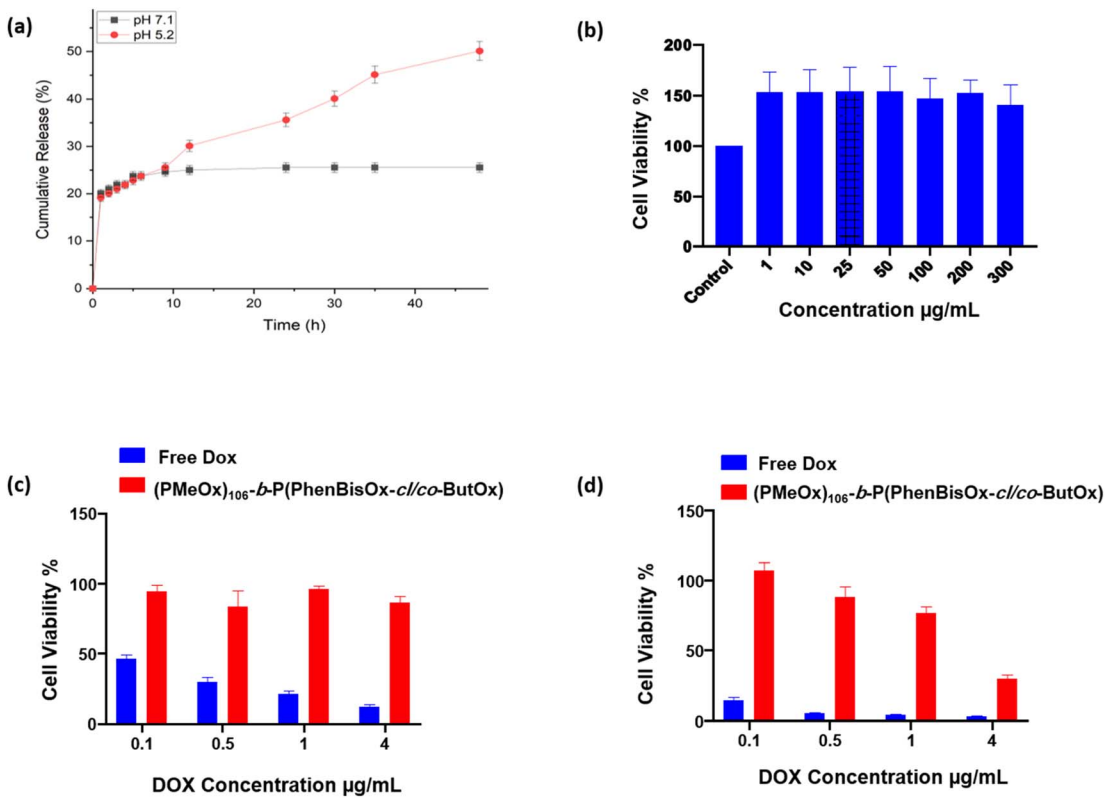

Fig. 4 *In vitro* studies of CCS POxs $(PMeOx)_{106}$-*b*-P(PhBisOx-*cl*/*co*-ButOx), (a) DOX release profile from CCS POxs in PBS at different pH values at 37 °C, (b) cell viability of HeLa cells with different concentrations of CCS POxs for 48 h, (c) cytotoxicity of DOX-loaded CCS POx and free DOX in HeLa cells for 24 h, and (d) cytotoxicity of DOX-loaded CCS POx and free DOX in HeLa cells for 48 h. The results are presented as average data with SD ($n = 2$) in triplicates.

observed on all CCS POxs when incubated for 24 and 48 h, which supports that they are potential drug carriers for drug delivery applications (Fig. S9 and S10, ESI†).

This study aims to use CCS POxs as a carrier of drugs. DOX was loaded onto CCS POxs to evaluate their drug delivery efficiency, and their cytotoxicity was studied and compared with free DOX. The HeLa cells were incubated with different concentrations (0.1 to 4 μg mL^{-1}) of each of the CCS POxs and free DOX for 24 and 48 h. The DOX-loaded CCS POxs showed no cytotoxic effect, whereas free DOX showed a cytotoxic effect in a concentration-dependent manner after 24 h as shown in (Fig. S11, ESI†). Fig. 4(c) and (d) show that the DOX-loaded CCS $(PMeOx)_{106}$-*b*-P(PhBisOx-*cl*/*co*-ButOx) exhibited a cytotoxic effect in a concentration-dependent manner after 24 h and 48 h, respectively, and free DOX appeared to show more than 75 to 95% cytotoxic effect. Another indicator of the slower DOX release is that after 48 h, CCS POxs loaded with DOX killed more cells than after 24 h (Fig. S12, ESI†). Overall, the results indicated that the effect is less toxic when DOX is encapsulated within the CCS POxs, which suggests that they are excellent biocompatible drug carriers for drug delivery applications.

Conclusion

In conclusion, a series of well-defined amphiphilic CCS $(PMeOx)_n$-*b*-P(PhBisOx-*cl*/*co*-ButOx)s were synthesized *via* the "arm first" strategy. The CCS POxs formed unimolecular micelles in water, as proven by DLS and TEM. The initial feed ratio of the hydrophobic monomer (PButOx) and cross-linker (PhBisOx) affects the size of the CCS polymer cores as well as the size of the corresponding micelles. The DLC and DLE increased when the hydrophobic core size increased, indicating that the encapsulation of DOX occurred *via* hydrophobic interaction. In addition, the *in vitro* study showed that the DOX-loaded CCS POxs released the DOX steadily over time under physiological conditions and that the DOX release was faster in an acidic environment. The cell viability experiments showed that the CCS POxs are biocompatible with cell viability ~100%, even at a concentration of 300 μg mL^{-1}. In contrast, the DOX-encapsulated CSS POxs exhibited a cytotoxic effect in HeLa cells. These results suggest that CCS POxs can indeed play a major role as nanoplatforms for drug and gene delivery applications.

Conflicts of interest

The authors declare no competing financial interest.

Acknowledgements

King Abdullah University of Science and Technology (KAUST) supported the research reported in this publication.

References

1 G. Liu and Z. An, Frontiers in the design and synthesis of advanced nanogels for nanomedicine, *Polym. Chem.*, 2014, **5**(5), 1559–1565.
2 A. Rösler, G. W. M. Vandermeulen and H.-A. Klok, Advanced drug delivery devices *via* self-assembly of amphiphilic block copolymers, *Adv. Drug Delivery Rev.*, 2012, **64**, 270–279.
3 K. Kita-Tokarczyk, J. Grumelard, T. Haefele and W. Meier, Block copolymer vesicles—using concepts from polymer chemistry to mimic biomembranes, *Polymer*, 2005, **46**(11), 3540–3563.
4 J. Xu, Q. Fu, J. M. Ren, G. Bryant and G. G. Qiao, Novel drug carriers: from grafted polymers to cross-linked vesicles, *Chem. Commun.*, 2013, **49**(1), 33–35.
5 R. K. O'Reilly, C. J. Hawker and K. L. Wooley, Cross-linked block copolymer micelles: functional nanostructures of great potential and versatility, *Chem. Soc. Rev.*, 2006, **35**(11), 1068–1083.
6 S. Peng, K. Wang, D.-S. Guo and Y. Liu, Supramolecular polymeric vesicles formed by *p*-sulfonatocalix[4]arene and chitosan with multistimuli responses, *Soft Matter*, 2015, **11**(2), 290–296.
7 E. G. Bellomo, M. D. Wyrsta, L. Pakstis, D. J. Pochan and T. J. Deming, Stimuli-responsive polypeptide vesicles by conformation-specific assembly, *Nat. Mater.*, 2004, **3**(4), 244–248.
8 C. Kojima, K. Kono, K. Maruyama and T. Takagishi, Synthesis of Polyamidoamine Dendrimers Having Poly(ethylene glycol) Grafts and Their Ability To Encapsulate Anticancer Drugs, *Bioconjugate Chem.*, 2000, **11**(6), 910–917.
9 S. Chen, X.-Z. Zhang, S.-X. Cheng, R.-X. Zhuo and Z.-W. Gu, Functionalized Amphiphilic Hyperbranched Polymers for Targeted Drug Delivery, *Biomacromolecules*, 2008, **9**(10), 2578–2585.
10 J. Liu, H. Duong, M. R. Whittaker, T. P. Davis and C. Boyer, Synthesis of functional core, star polymers *via* RAFT polymerization for drug delivery applications, *Macromol. Rapid Commun.*, 2012, **33**(9), 760–766.
11 K. Knop, G. M. Pavlov, T. Rudolph, K. Martin, D. Pretzel, B. O. Jahn, D. H. Scharf, A. A. Brakhage, V. Makarov, U. Möllmann, F. H. Schacher and U. S. Schubert, Amphiphilic star-shaped block copolymers as unimolecular drug delivery systems: investigations using a novel fungicide, *Soft Matter*, 2013, **9**(3), 715–726.
12 K. Knop, D. Pretzel, A. Urbanek, T. Rudolph, D. H. Scharf, A. Schallon, M. Wagner, S. Schubert, M. Kiehntopf, A. A. Brakhage, F. H. Schacher and U. S. Schubert, Star-Shaped Drug Carriers for Doxorubicin with POEGMA and POEtOxMA Brush-like Shells: A Structural, Physical, and Biological Comparison, *Biomacromolecules*, 2013, **14**(8), 2536–2548.
13 A. D. Morara and R. L. McCarley, Encapsulation of Neutral Guests by Tri(ethylene oxide)-pyrrole-Terminated Dendrimer Hosts in Water, *Org. Lett.*, 2006, **8**(10), 1999–2002.
14 J. T. Wiltshire and G. G. Qiao, Recent Advances in Star Polymer Design: Degradability and the Potential for Drug Delivery, *Aust. J. Chem.*, 2007, **60**(10), 699–705.
15 L. Plet, G. Delecourt, M. Hanafi, N. Pantoustier, G. Pembouong, P. Midoux, V. Bennevault and P. Guégan,

Controlled star poly(2-oxazoline)s: synthesis, characterization, *Eur. Polym. J.*, 2020, **122**, 109323.
16 J. Huang, Z. Xiao, H. Liang and J. Lu, Star graft copolymer *via* grafting-onto strategy using a combination of reversible addition–fragmentation chain transfer arm-first technique and aldehyde–aminooxy click reaction, *Polym. Int.*, 2014, **63**(6), 1122–1128.
17 A. Blencowe, J. F. Tan, T. K. Goh and G. G. Qiao, Core cross-linked star polymers *via* controlled radical polymerisation, *Polymer*, 2009, **50**(1), 5–32.
18 J. M. Ren, T. G. McKenzie, Q. Fu, E. H. H. Wong, J. Xu, Z. An, S. Shanmugam, T. P. Davis, C. Boyer and G. G. Qiao, Star Polymers, *Chem. Rev.*, 2016, **116**(12), 6743–6836.
19 T. K. Georgiou, Star polymers for gene delivery, *Polym. Int.*, 2014, **63**(7), 1130–1133.
20 W. Wu, W. Wang and J. Li, Star polymers: advances in biomedical applications, *Prog. Polym. Sci.*, 2015, **46**, 55–85.
21 T. Kagiya, S. Narisawa, T. Maeda and K. Fukui, Ring-opening polymerization of 2-substituted 2-oxazolines, *J. Polym. Sci., Part B: Polym. Lett.*, 1966, **4**(7), 441–445.
22 D. A. Tomalia and D. P. Sheetz, Homopolymerization of 2-alkyl- and 2-aryl-2-oxazolines, *J. Polym. Sci., Part A-1: Polym. Chem.*, 1966, **4**(9), 2253–2265.
23 T. G. Bassiri, A. Levy and M. Litt, Polymerization of cyclic imino ethers. I. Oxazolines, *J. Polym. Sci., Part B: Polym. Lett.*, 1967, **5**(9), 871–879.
24 W. Seeliger, E. Aufderhaar, W. Diepers, R. Feinauer, R. Nehring, W. Thier and H. Hellmann, Recent Syntheses and Reactions of Cyclic Imidic Esters, *Angew. Chem., Int. Ed. Engl.*, 1966, **5**(10), 875–888.
25 B. Verbraeken, B. D. Monnery, K. Lava and R. Hoogenboom, The chemistry of poly(2-oxazoline)s, *Eur. Polym. J.*, 2017, **88**, 451–469.
26 B. Guillerm, S. Monge, V. Lapinte and J. J. Robin, How to Modulate the Chemical Structure of Polyoxazolines by Appropriate Functionalization, *Macromol. Rapid Commun.*, 2012, **33**(19), 1600–1612.
27 O. Sedlacek, A. Van Driessche, A. Uvyn, B. G. De Geest and R. Hoogenboom, Poly(2-methyl-2-oxazoline) conjugates with doxorubicin: from synthesis of high drug loading water-soluble constructs to *in vitro* anti-cancer properties, *J. Controlled Release*, 2020, **326**, 53–62.
28 Z. Ahmad, A. Shah, M. Siddiq and H.-B. Kraatz, Polymeric micelles as drug delivery vehicles, *RSC Adv.*, 2014, **4**(33), 17028–17038.
29 B. Daglar, E. Ozgur, M. E. Corman, L. Uzun and G. B. Demirel, Polymeric nanocarriers for expected nanomedicine: current challenges and future prospects, *RSC Adv.*, 2014, **4**(89), 48639–48659.
30 R. Hoogenboom, M. W. M. Fijten, H. M. L. Thijs, B. M. van Lankvelt and U. S. Schubert, Microwave-assisted synthesis and properties of a series of poly(2-alkyl-2-oxazoline)s, *Des. Monomers Polym.*, 2005, **8**(6), 659–671.
31 M. W. M. Fijten, R. Hoogenboom and U. S. Schubert, Initiator effect on the cationic ring-opening copolymerization of 2-ethyl-2-oxazoline and 2-phenyl-2-oxazoline, *J. Polym. Sci., Part A: Polym. Chem.*, 2008, **46**(14), 4804–4816.
32 R. Luxenhofer, Y. Han, A. Schulz, J. Tong, Z. He, A. V. Kabanov and R. Jordan, Poly(2-oxazoline)s as Polymer Therapeutics, *Macromol. Rapid Commun.*, 2012, **33**(19), 1613–1631.
33 G. Hayes, B. Drain and C. R. Becer, Multiarm Core Cross-Linked Star-Shaped Poly(2-oxazoline)s Using a Bisfunctional 2-Oxazoline Monomer, *Macromolecules*, 2022, **55**(1), 146–155.
34 K. Aoi and M. Okada, Polymerization of oxazolines, *Prog. Polym. Sci.*, 1996, **21**(1), 151–208.
35 Y. Chujo, K. Sada, K. Matsumoto and T. Saegusa, Synthesis of nonionic hydrogel, lipogel, and amphigel by copolymerization of 2-oxazolines and a bisoxazoline, *Macromolecules*, 1990, **23**(5), 1234–1237.
36 O. Tacar, P. Sriamornsak and C. R. Dass, Doxorubicin: an update on anticancer molecular action, toxicity and novel drug delivery systems, *J. Pharm. Pharmacol.*, 2013, **65**(2), 157–170.
37 H. Kheiri Manjili, P. Ghasemi, H. Malvandi, M. S. Mousavi, E. Attari and H. Danafar, Pharmacokinetics and *in vivo* delivery of curcumin by copolymeric mPEG-PCL micelles, *Eur. J. Pharm. Biopharm.*, 2017, **116**, 17–30.